Exact Topological Quantum Order in $D = 3$ and Beyond: Branyons and Brane-Net Condensates

H. Bombin and M.A. Martin-Delgado
Departamento de Física Teórica I, Universidad Complutense, 28040. Madrid, Spain.

We construct an exactly solvable Hamiltonian acting on a 3-dimensional lattice of spin-$\frac{1}{2}$ systems that exhibits topological quantum order. The ground state is a string-net and a membrane-net condensate. Excitations appear in the form of quasiparticles and fluxes, as the boundaries of strings and membranes, respectively. The degeneracy of the ground state depends upon the homology of the 3-manifold. We generalize the system to $D \geq 4$, were different topological phases may occur. The whole construction is based on certain special complexes that we call colexes.

PACS numbers: 11.15.-q, 71.10.-w

I. INTRODUCTION

Deviations from a standard theory in a certain field of Physics has always attracted the attention of searching for new physics. In condensed matter, the standard model is the Landau Theory of quantum liquids (Fermi liquid) supplemented with the Spontaneous Symmetry Breaking mechanism (SBB) and the Renormalization Group scheme [1], [2], [3]. The concept of local order parameter plays a central role in detecting quantum phases or orders within Landau's theory. Quite on the contrary, topological orders cannot be described by means of local order parameters or long range interactions. Instead, a new set of quantum numbers is needed for this new type of phases, such as ground state degeneracy, quasiparticle braiding statistics, edge states [4], [5], [6], topological entropy [7], [8], etc.

A consequence of the SBB is the existence of a ground state degeneracy. However, in a topological order there exists ground state degeneracy with no breaking of any symmetry. This degeneracy has a topological origin. Thus, topological orders deviate significantly from more standard orders covered within the Landau symmetry-breaking theory. The existence of topological orders seems to indicate that nature is much richer than the standard theory has predicted so far.

Emblematic examples of topological orders are Fractional Quantum Hall Liquids (FQH). FQH systems contain many different phases at T=0 which have the same symmetry. Thus, those phases cannot be distinguished by symmetries and Landau's SBB does not apply [4], [9], [10], [11]. Then, we need to resort to other types of quantum numbers to characterize FQH liquids. For example, the ground state degeneracy d_g depends on the genus g of the $D = 2$ surface where the electron system is quantized, namely, $d_g = m^g$ with filling factor being $\nu = \frac{1}{m}$.

There are several other examples of topological orders like short range RVB (Resonating Valence Bond) models [12], [13], [14], [15], quantum spin liquids [16], [17], [5], [18], [19], [20], [21], [22], [23] etc. Due to this topological order, these states exhibit remarkable entanglement properties [24], [25]. Besides these physical realizations, there have been other proposals for implementing topological orders with optical lattices [26], [27], [28] with spin interactions in honeycomb lattices [29]. In this paper we shall be concerned with topological models constructed with spins $S = \frac{1}{2}$ located at the sites of certain lattices with coordination number, or valence, depending on the dimension D of the space and the property of being coloreable to be explained in Sect.II.

From the point of view of quantum information [30], a topological order is a new type of entanglement: it exhibits non-local quantum correlations in quantum states. A topological phase transition is a change between quantum states with different topological orders. In dimensions $D \geq 4$ we construct exact examples of quantum lattice Hamiltonians exhibiting topological phase transitions in Sect.IV A. Here we find an example of topology-changing transition as certain coupling constant is varied in $D = 4$. This is rather remarkable since the most usual situation is to have an isolated topological point or phase surrounded by non-topological phases [24], [25].

In two dimensions, a large class of "doubled" topological phases has been described and classified mathematically using the theory of tensor categories [47]. The physical mechanism underlying this large class of topological orders is called string-net condensation. This mechanism is the equivalent mechanism to particle condensation in the emergence of ordered phases in Landau's theory. A string-net is a network of strings and it is a concept more general than a collection of strings, either closed or open. In a string-net we may have the situation in which a set of strings meet at a branching point or node, something that is missing in ordinary strings which have two ends at most (see Fig.12). More specifically, the ground state of these theories are described by superpositions of states representing string-nets. The physical reason for this is the fact that local energy constraints can cause the local microscopic degrees of freedom present in the Hamiltonian to organize into effective extended objects like string-nets.

A new field of applications for topological orders has emerged with the theory of quantum information and computation [31], [32], [33], [34]. Quantum computation, in a nutshell, is the art of mastering quantum phases to encode and process information. However, phases of

quantum states are very fragile and decohere. A natural way to protect them from decoherence is to use topologically ordered quantum states which have a non-local kind of entanglement. The non-locality means that the quantum entanglement is distributed among many different particles in such a way that it cannot be destroyed by local perturbations. This reduces decoherence significantly. Moreover, the quantum information encoded in the topological states can be manipulated by moving quasiparticle excitations around one another producing braiding effects that translate into universal quantum gates [31], [35], [36], [37], [38], [39]. Nevertheless, there are also alternative schemes to do lots of quantum information tasks by only using the entanglement properties of the ground state [40], [41], [42].

The situation for topological orders in $D = 3$ is less understood. This is in part due to the very intrincate mathematical structure of topology in three dimensions. While the classification of all different topologies is well stablished in two dimensions, in $D = 3$ the classification is much more difficult and only recently it appears to be settled with the proof of the Thurston's geometrization conjecture [43], a result that includes the Poincaré conjecture as a particular case [44], [45], [46]. Topological orders have been investigated in three dimensions with models that exhibit string-net condensation [47] using trivalent lattices that extend the case of trivalent lattices in two dimensions. However, a problem arises when one wishes to have an exactly solvable Hamiltonian describing this topological phase since this type of magnetic flux operators do not commute in three dimensions any more. A solution to this problem can be found by imposing additional constrains to the mechanism found in $D = 2$, but this obscures somehow the geometrical picture of the resulting exactly solvable model. Alternatively, it is possible to use a 3D-generalization of Kitaev's toric code to provide examples with topological order based both in string condensation and membrane condensation [48]. In the theory of topological quantum error correcting codes, there are also studies of toric codes in dimensions higher than $D = 2$ [33], [49], [50].

In this paper we introduce a new class of exactly solvable models in $D = 3$ that exhibits topological order. Here we construct a class of models in which magnetic flux operators of several kinds commute among each other. This is achieved by requiring certain geometrical properties to the lattices where the models are defined on. As a result, we can study the whole spectrum of the models and in particular their quantum topological properties. The ground state can be described as a string-net condensate or alternatively, as a membrane-net condensate. A membrane-net condensate is a generalization of a collection of membranes, much like string-nets generalize the notion of strings. Thus, in a membrabrane-net, membranes can meet at branching lines instead of points. Excitations come into two classes: there are quasiparticles that appear as the end-points of strings, or certain type of fluxes that appear as the boundaries of membranes. These fluxes are extended objects. Interestingly enough, when a quasiparticle winds around a closed flux, the system picks up a non-trivial Abelian phase (see Fig.15), much similar like when one anyon [51], [52] winds around another anyon acquiring an Abelian factor in the wave function of the system. We coin the name branyons to refer to this quasiparticles that are anyons with an extended structure. In fact, in our models they appear as Abelian branyons.

Our constructions can be nicely generalized to higher dimensions and we can compute exactly the ground state degeneracies in terms of the Betti numbers of the manifolds where the lattice models are defined. This allows us to discriminate between manifolds with differente homological properties using quantum Hamiltonians. The generalized membranes are called branes and we find also a brane-net mechanism.

This paper is organized as follows: in Sect.II we introduce the models defined in three dimensional lattices placed on different manifolds. These lattices are constructed by means of color complexes that we call colexes of dimension 3, or 3-colexes; in Sect.III the notion of colexes is generalized to arbitrary dimensions; in Sect.IV we extend the topological quantum Hamiltonians beyond $D = 3$ dimensions and in particular we find instances of topology-changing phase transitions; Sect.V is devoted to conclusions. In a set of appendices we provide a full account of technical details pertaining to particular aspects of our models.

II. THE MODEL IN 3-MANIFOLDS

A. Topological order and homology

The model that we are going to study belongs to the category of topologically ordered quantum systems. A system with topological quantum order is a gapped system that shows a dependency between the degeneracy of its ground state and the topology of the space where it exists. Certainly such a dependency could manifest in many ways, typically as a function of certain topological invariants of the space.

In the case at hand these topological invariants turn out to be the Betti numbers of the manifold. These in turn reflect the $\mathbf{Z}_2$-homology [42] of the manifold, and so we will now introduce very naively several concepts and illustrate them using a well known 3-manifold, the 3-torus.

Consider any 3-manifold $\mathcal{M}$. For a 1-cycle we understand any closed non-oriented curve γ in it, or several such curves. In other words, it is a closed 1-manifold embedded in $\mathcal{M}$. Suppose that we can embed in $\mathcal{M}$ a 2-manifold in such a way that its boundary is γ. In that case γ is called a 1-boundary and said to be homologous to zero. More generally consider two non-oriented curves γ_1 and γ_2 with common endpoints, as in Fig. 1 (a). We can combine these two curves into a single 1-cycle, and

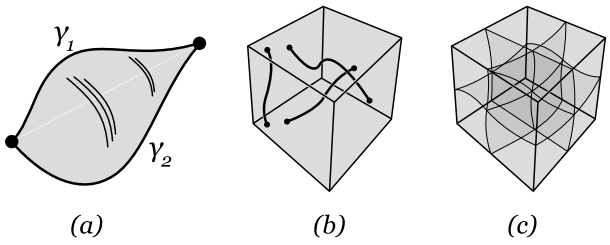

FIG. 1: In (a) the two curves are homologous because they form the boundary of a deformed disc. In (b) and (c) the 3-torus is represented as a cube in which opposite sides must be identified. In (b) it is shown a basis for 1-cycles and in (c) a basis for 2-cycles.

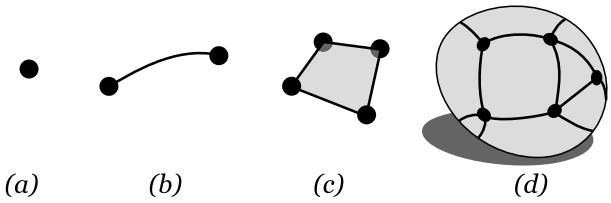

FIG. 2: A vertex (a), an edge (b), a face (c) and a polyhedral solid (d).

then we say that they are homologous if the 1-cycle is a 1-boundary. In other words $\gamma_1 \sim \gamma_2$ iff $\gamma_1 + \gamma_2 \sim 0$. This kind of equivalence can also be applied to two 1-cycles, and thus two 1-cycles are homologous iff their combination is a 1-boundary. Then the idea is that any 1-cycle can be constructed, up to homology equivalence, by combination of certain basic 1-cycles. The number of 1-cycles needed to form such a basis is a topological invariant, the first Betti number h_1 of the manifold $\mathcal{M}$. For the 3-torus $h_1 = 3$. A possible basis in this case is the one formed by the three 1-cycles that cross the torus in the three spatial directions, as in fig. 1 (b).

Similarly we can think in 2-cycles as closed 2-manifolds embedded in $\mathcal{M}$. Then, when a 2-cycle is the boundary of some embedded 3-manifold it is called a 2-boundary and said to be homologous to zero. Two 2-manifolds with common boundary can be sewed together to form a 2-cycle, and they are homologous if this 2-cycle is a 2-boundary. As in the case of 1-cycles, there exist a basis for 2-cycles up to homology. Again these can be exemplified in the case of a 3-torus, see Fig. 1(c). The topological invariant that gives the cardinality of such a basis is the second Betti number h_2 and equals h_1.

Throughout the text we use sometimes a more suggestive language. Instead of curves we will talk about strings, closed or open with endpoints. Similarly, we will refer to embedded 2-manifolds as membranes, either closed or with a boundary.

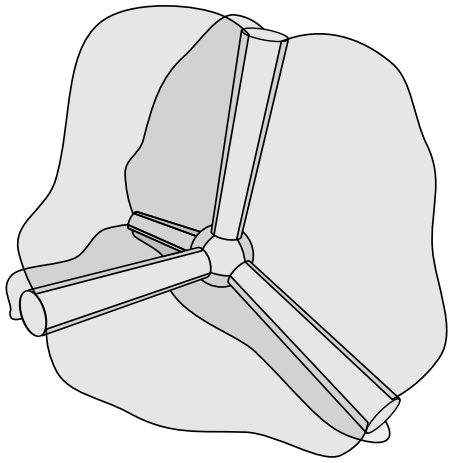

FIG. 3: The neighborhood of a vertex in a 3-colex. 4 edges, 6 faces and 4 cells meet at each vertex.

B. System and Hamiltonian

Consider a 3-dimensional closed connected manifold M that has been constructed by gluing together polyhedral solids. These polyhedral solids are balls whose boundary surface is a polyhedron, i.e., a sphere divided into faces, edges and vertices, see Fig. 2. This gluing of polyhedral solids must respect this structure. For brevity we will call polyhedral solids simply as cells. Thus we have a 3-manifold divided into vertices V, edges E, faces F and cells C. Such a structure in a 3-manifold is called a 3-complex.

In order to construct the topogical quantum system that we propose, we consider a 3-complex such that
i) the neighborhood of every vertex is as the one in Fig. 3 and
ii) cells are four-colored, in such a way that adjacent cells have different colors.
The colors we shall use are red, green, blue and yellow (r,g,b,y). With these assumptions we will proceed to color edges and faces, and finally we will see that the whole structure of the manifold is contained in the coloring of the edges.

With a glance at Fig. 3 we see that the four cells meeting at each vertex must have different colors. In the figure we also see that each edge lyes in three cells of different colors. Then each of the endpoints of the edge is in the corner of a cell of a fourth color, so that we can say that it connects two cells of the same color. We proceed to label edges with the color of the cells they connect, see figure Fig. 4 (b). As a result, the four edges that meet at a vertex have all different colors, see Fig. 4 (a). Also, the edges lying on a r-cell are not r-edges. But much more is true. Consider a r-cell c, and any vertex v in its boundary. The red edge that ends in v does not lye on the cell c, so that the other three edges incident in v do. But then any connected collection of g-, b- and y-edges corresponds exactly to the set of edges of some r-cell.

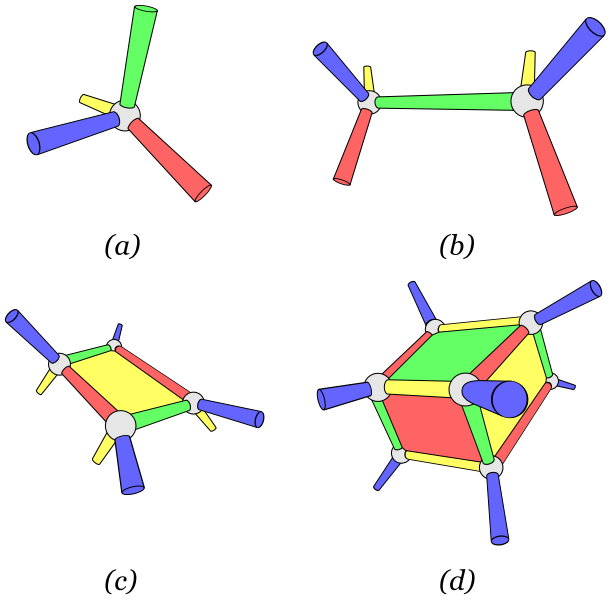

FIG. 4: Neighborhoods in a 3-colex of a vertex (a), a g-edge (b), a by-face, with the yellow side visible and the blue one hidden (c) and a b-cell (d). Faces are colored according to the color of the cell at their visible side.

We label faces with two colors. If a face lyes between a p-cell and a q-cell, we say that it is a pq-face, see Fig. 4 (c). Then consider for example a ry-cell. Since neither r- nor y-edges can lye on its boundary, this must consist of a sequence of alternating b- and g-edges. Conversely, any such path is the boundary of some ry-face. To check this, first note that exactly one such path traverses any given g-edge e. But e must lye exactly on one ry-face, the one that separates the r- and the y-cell it lyes on.

As promised, we have shown that the entire structure of the manifold is contained in two combinatorial data: the graph and the colors of its edges. We call the resulting structure a 3-colex, for color complex in a 3-manifold. The simplest example of such a 3-colex with non-trivial homology is displayed in Fig. 5. It corresponds to the projective space P^3. In appendix B we will give a procedure to construct a colex of arbitrary dimension D, or D-colex, starting with an arbitrary complex in a D-manifold.

We now associate a physical system to the 3-colex. To this end, we place at each vertex (site) a spin-$\frac{1}{2}$ system. To each cell c, we attach the cell operator

$$B_c^X := \bigotimes_{i\in I_c} X_i, \tag{1}$$

where X_i is the Pauli σ_1 matrix acting on site i and I_c is the set of sites lying on the cell. Similarly, to each face f we attach the face operator

$$B_f^Z := \bigotimes_{i\in I_f} Z_i, \tag{2}$$

where Z_i is the Pauli σ_3 matrix acting in site i and I_f is the set of sites lying on the face. We have

$$\forall\, c \in C, f \in F, \qquad [B_c^X, B_f^Z] = 0. \tag{3}$$

To show this, consider any cell c and face f. The edges of c come in three colors and the edges of f in two. Thus they have a least a common color, say q. Given any shared vertex, we consider its q-edge e. But e lyes both on c and f, and thus its other endpoint is also a shared vertex. Therefore c and f share an even number of vertices and $[B_c^X, B_f^Z] = 0$.

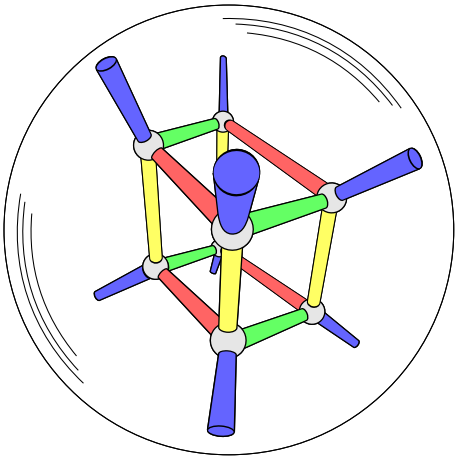

FIG. 5: The projective space P^3 can be obtained starting with a solid sphere and identifying opposite points in its surface. Here we use such a representation to show a 3-colex in P^3.

The Hamiltonian that we propose is constructed by combining cell and face operators:

$$H = -\sum_{c\in C} B_c^X - \sum_{f\in F} B_f^Z \tag{4}$$

Observe that color plays no role in the Hamiltonian, rather, it is just a tool we introduce to analyze it. In appendix D we calculate the degeneracy of the ground state. It is 2^k with

$$k = 3h_1, \tag{5}$$

and therefore depends only upon the manifold, which is a signature of topological quantum order.

The ground states $|\psi\rangle$ are characterized by the conditions

$$\forall\, c \in C \qquad B_c^X|\psi\rangle = |\psi\rangle, \tag{6}$$

$$\forall\, f \in F \qquad B_f^Z|\psi\rangle = |\psi\rangle, \tag{7}$$

for cell and face operators. Those eigenstates $|\psi'\rangle$ for which any of the conditions is violated is an excited state. There are two kinds of excitations. If $B_c^X|\psi'\rangle = -|\psi'\rangle$ we say that there is an excitation at cell c. Similarly, if $B_f^Z|\psi'\rangle = -|\psi'\rangle$ then the face f is excited. Below we will show that cell excitations are related to quasiparticles and face excitations to certain flux. For know we are just

interested in noting that excitations have a local nature and thus the Hamiltonian (4) is gapped. Then since the ground state degeneracy depends upon the topology, we have topological quantum order.

C. Strings and Membranes

From this point on we shall pursue a better understanding both the ground state degeneracy and the excitations by means of the introduction of string and membrane operators. In this direction, an essential notion will be that of a *shrunk complex*, both of the first and second kind. The motivation after the construction of these complexes from the colexes is that only at the shrunk complex level it is possible to visualize neatly the strings and membranes that populate the model. These new shrunk complexes are not colexes, but its cells are associated to cells in the colex, and thus have color labels.

1. *Shrunk complex of the first kind*

It is associated to a color, and it allows to visualize strings of that particular color. Consider for example the b-shrunk complex. The idea is that we want to keep only b-edges, whereas g-,r- and y-edges get shrunk and disappear. To this end, we start placing a vertex at each b-cell and connecting them through edges, which are in one to one correspondence with b-edges. Then we have to place the faces of the new complex, and they correspond to rg-, ry- and gy-faces. In particular, consider a rg-face. It has b- and g-edges, but after g-edges are shrunk only b-edges remain. Finally we need cells. They come from g-, r- and y-cells. In particular, consider a g-cell. It has r-, y- and b-edges, but only b-edges are retained. Similarly, it has gb-, gr- and gy-faces, but we keep only gb-faces. See Fig. 6 (c) for an example an also Fig. 7.

Now consider any path, closed or not, in the b-shrunk complex. We call such a path a b-string. Recall that each edge of a shrunk complex corresponds to a b-edge in the 3-colex. Thus at the colex level a b-string is a collection of b-edges that connect b-cells, see Fig. 7 (a). Each b-edge contains two vertices. Then to each b-string s we can associate an operator $B_s^Z = \bigotimes_{i\in I_s} Z_i$, where I_s is the set of vertices lying in the string.

As shown in Fig. 7 (b), the operator B_f^Z of a yr-face corresponds to a closed b-string s. This string is the boundary of the corresponding face in the b-shrunk complex. As an operator, B_s^Z clearly commutes with the Hamiltonian and acts trivially on the ground state (6).

In fact, any closed string gives rise to a string operator that commutes with the Hamiltonian(4). If the string is homologous to zero the corresponding string operator acts trivially on the ground state. In order to understand this, consider a closed red string homologous to zero. It must be a combination of boundaries of faces. Then the string operator is the product of the operators

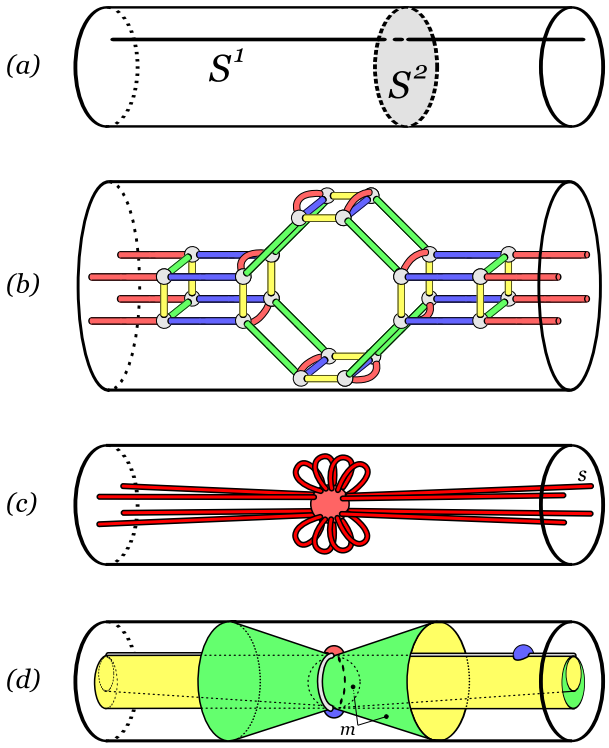

FIG. 6: (a) A representation of the space $S^2 \times S^1$. Each section of the solid tube is a sphere, and both ends of the tube are identified. (b) A 3-colex in $S^2 \times S^1$. It consists of 24 vertices, 12 edges of each color, 4 br-faces, 8 by-faces, 6 rg-faces, 4 ry-faces, 4 gy-faces, 2 b-cells, 1 r-cell, 3 g-cells and 2 y-cells. (c) The r-shrunk complex of the previous colex. The vertex corresponds to a r-cell, and edges to r-edges. An example of closed string is the edge marked with a s. It has nontrivial homology. (d) The gy-shrunk complex of the previous colex. Vertices correspond to b- and r-cells, edges to rb-faces, face to gy-faces and cells to g- and y-cells. An example of a closed membrane is the combination of the faces marked with a m. This membrane has nontrivial homology.

of these faces. Similarly, the action of two string operators derived from homologous strings of the same color is identical on the ground state. Therefore it makes sense to label the string operators as S_μ^p, where p is a color and μ is a label denoting the homology of the string.

2. *Shrunk complex of the second kind*

It is associated to two colors, and it allows the visualization of certain membranes, as we explain now. Let us consider for example the ry-shrunk complex. The idea is that we want to keep only ry-faces, whereas the rest of faces get shrunk and disappear. This time vertices correspond to b- and g-cells. Edges come from bg-faces. A bg-face lyes between a g- and a b-cell, and the corresponding edge will connect the vertices coming from these cells. We have already mentioned that the faces of the ry-shrunk complex come from ry-faces in the colex,

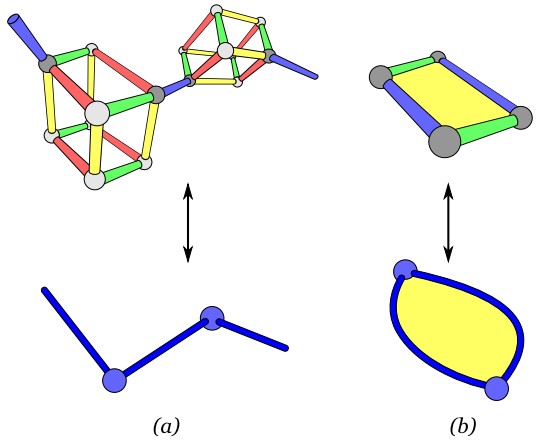

FIG. 7: In this figure the top represents part of a colex and the bottom the corresponding portion of the b-shrunk complex. Vertexes in the b-shrunk complex come from b-cells in the colex, edges from b-edges, faces from ry-, rg- and gy-faces and cells from r-, y- and g-cells. (a) A b-string. In the colex it is a collection of b-edges linking b-cells. In the b-shrunk complex the path of edges can be clearly seen. (b) A ry-face corresponds to a face in the b-shrunk complex, and thus its boundary can be viewed as a b-string.

but we have to explain how they are attached. Observe that each ry-face has certain amount of adjacent gb-faces. Here for adjacent objects we will only mean that their intersection is not empty. In particular there is a gb-face at each of the vertices of the ry-face. Then the face in the complex has in its perimeter the edges coming from its adjacent gb-faces. Finally we have to consider cells, which come from r- and y-cells and only keep their ry faces. So in the boundary of a cell coming from an r-cell we see vertices from adjacent b- and g-cells, edges from adjacent bg-faces and faces from ry-faces in the boundary of the r-cell. See Fig. 6 (d) and Fig. 8.

Now consider any membrane, that is, a connected collection of faces, closed or with a boundary, in the ry-shrunk complex. We call such a membrane m a ry-membrane, see Fig. 6 (d) and Fig. 8 (a). We can associate an operator B_m^X to it. It is the product of the B_f^X operators of the corresponding ry-faces in the colex.

As shown in Fig. 8 (b), the operator B_c^X of a r-cell c correspond to a closed ry-membrane m. This membrane is the boundary of the corresponding cell in the ry-shrunk complex. As an operator, B_m^X clearly commutes with the Hamiltonian and acts trivially on the ground state (7).

In complete analogy with strings, any closed membrane gives rise to a membrane operator that commutes with the Hamiltonian. If the membrane is homologous to zero then the corresponding membrane operator acts trivially on the ground state. Similarly, the action of two string operators derived from homologous membranes of the same color is identical on the ground state, and we label membrane operators as M_μ^{pq}, where p and q are colors and μ is a label denoting the homology of the membrane.

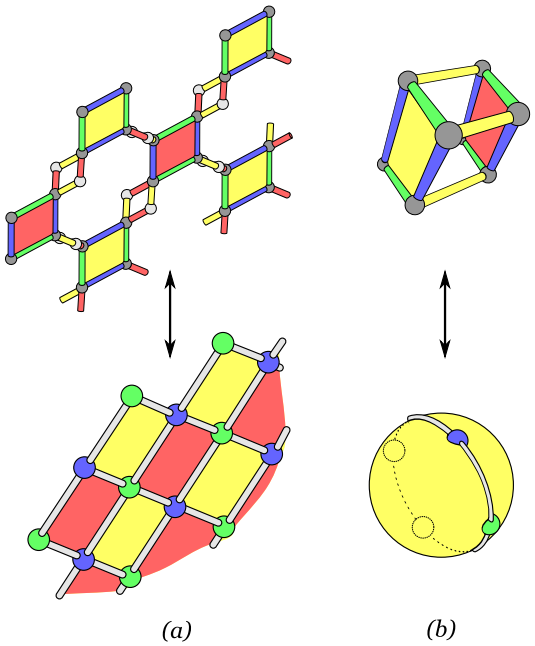

FIG. 8: In this figure the top represents part of a colex and the bottom the corresponding portion of the ry-shrunk complex. Vertexes in the ry-shrunk complex come from g- and b-cells in the colex, edges from gb-faces, faces from ry-faces and cells from r- and y-cells.(a) A ry-membrane. In the colex it is a collection of ry-faces linked by gb-faces. In the ry-shrunk complex the brane can be clearly seen (b) A r-cell corresponds to a cell in the ry-shrunk complex, and thus its boundary can be viewed as a ry-membrane.

3. *Commutation rules*

We will now consider the commutation rules between string and membrane operators. We first consider the case of a membrane and a string with no common color in their labels. As displayed in figure Fig. 8(a), a rg-membrane is made up of g- and b-edges. Then for the same argument of (3) we have

$$\forall\, \mu, \nu \qquad [M_\mu^{rg}, S_\nu^b] = 0, \tag{8}$$

and analogously for any combination of three different colors. More interesting is the case in which there is a shared color. As displayed in Fig. 9, at each place where a p-string crosses a pq-membrane they have a site in common. Thus, if the labels μ and ν are such that a ν string crosses a μ membrane an odd number of times, we have

$$\{M_\mu^{pq}, S_\nu^p\} = 0. \tag{9}$$

In other case, that is, if they cross an even number of times, the operators commute.

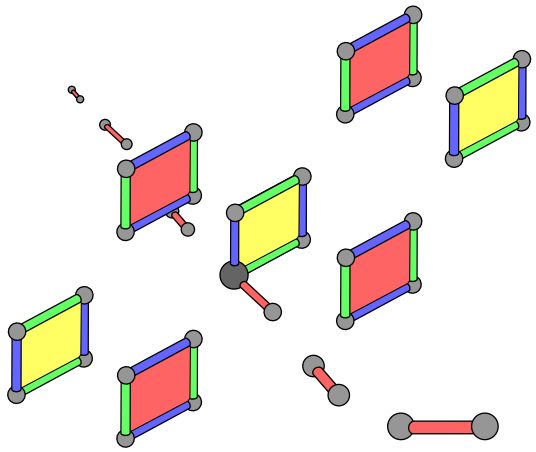

FIG. 9: When a r-string s crosses a ry-membrane m, they meet at a vertex. In terms of string and membrane operators, this means that B_m^X and B_s^Z act in a common site.

D. Ground state

Above we have discussed how the action of string or membrane operators on the ground state depends only upon their homology. It is in this sense that homologous strings or membranes give rise to equivalent operators. This equivalence however can be extended to take color into account, and we say that two membrane or string operators are equivalent if they are equal up to combinations with cell and face operators. Then, as we prove for general D in appendix C, we have the following interplay between homology and color:

$$S_\mu^r S_\mu^g S_\mu^b S_\mu^y \sim 1, \tag{10}$$

$$M_\mu^{pq} M_\mu^{qo} M_\mu^{op} \sim 1, \tag{11}$$

where o, p and q are distinct colors.

If we take all the r-, g- and b-strings for a given homology basis of 1-cycles, we obtain a complete set of compatible observables for the ground state subspace: any other string operator is equivalent to a combination of these strings, and no membrane operator that acts nontrivially in the ground state can commute with all of them. This is in fact why the number 3 appears in (5). As an example, a string basis in $S^2 \times S^1$ is displayed in Fig. 10 (a).

Similarly, if we take all the ry-, gy- and by-membranes for a given homology basis of 2-cycles, we obtain a complete set of compatible observables for the ground state subspace: any other membrane operator is equivalent to a combination of these membranes, and no string operator that acts nontrivially in the ground state can commute with all of them. A membrane basis in $S^2 \times S^1$ is displayed in Fig. 10 (b).

Observe that only those string operators that have nontrivial homology, that is, which act in a global manner in the system, are capable of acting nontrivially in the ground state whereas living it invariant. This is the signature of a string condensate, as introduced in [48]. Then it would be tempting to let S_b be the set of all boundary strings and try to write a ground state as

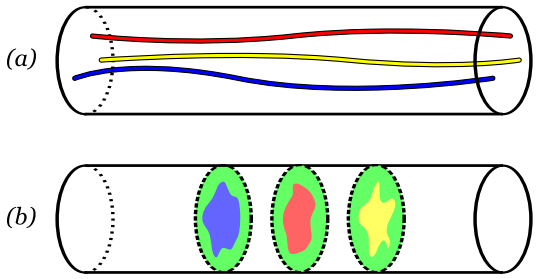

FIG. 10: Here we represent $S^2 \times S^1$ as in Fig. 6. In (a) it is shown a basis for nontrivial closed strings. The other possible such string is green, but it is a combination of these ones (10). (b) A membrane basis in $S^2 \times S^1$. We have chosen a gb, a gr and a gy-membrane. There are three other nontrivial membranes, in particular a br-, a by- and a yr-membrane, but they are combinations of these ones (11).

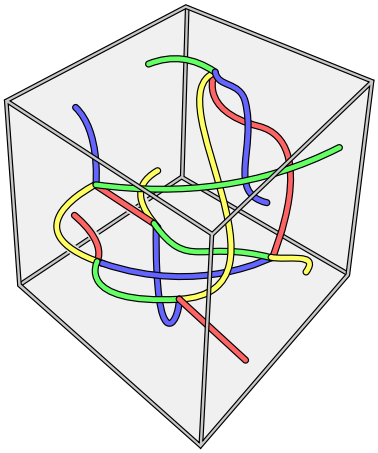

FIG. 11: The ground state of the system is a string-net condensate. This picture represents in a 3-torus a typical element of the sumation (13).

$$\sum_{s\in S_b} B_s^Z |\rightarrow\rangle^{\otimes |V|}, \tag{12}$$

where $|\rightarrow\rangle^{\otimes |V|}$ is the state with all spins pointing in the positive x direction. However, this fails. In fact, what we have is a *string-net condensate* [47] because, as indicated by (10), we can have branching points in which one string of each color meet. This means that the ground state is a superposition of all possible nets of strings, as depicted in Fig. 11. The correct way to write an example of a ground state is

$$\sum_{f\in F}(1+B_f^Z)|\rightarrow\rangle^{\otimes |V|} =: \sum_{\text{string-nets}} B_s^Z |\rightarrow\rangle^{\otimes |V|}. \tag{13}$$

We can state all of the above also in the case of membranes, and thus we should speak of a *membrane-net condensate*, and interestingly enough, in other topological

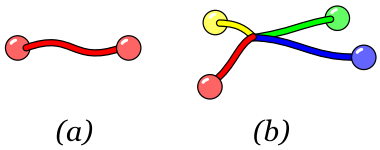

FIG. 12: There are two ways in which quasiparticles can be created locally. We can either create them by pairs of the same color forming a string (a) or in groups, one of each color forming a string-net (b).

orders in $D = 3$ based on toric codes do not exhibit a condensation of membrane-nets [48]. It is a membrane condensate because only membranes with nontrivial homology can act nontrivially in the ground state. And it is a net because, for example, as indicated by (11) a gr-, a gb- and a br-membrane can combine along a curve. Then if we let $|\uparrow\rangle^{\otimes|V|}$ denote the state with all spins up, the following is an example of a ground state:

$$\sum_{c\in C}(1+B_c^X)|\uparrow\rangle^{\otimes|V|} =: \sum_{\text{membrane-nets}} B_m^X|\uparrow\rangle^{\otimes|V|}. \quad (14)$$

E. Excitations

We now focus on excitations from the point of view of string and membrane operators. We can have two kinds of excitations, depending on wether a cell or face condition is violated. We start by considering excitations in r-cells, for example. Let $|\psi\rangle$ be a ground state and let S_{ij}^r be an open string operator connecting the cells i and j. The state $S_{ij}^r|\psi\rangle$ is an excited state. The excitations live precisely at cells i and j, and we call them quasiparticles with r-charge. Why should be color be considered a charge? We have the following 3 constraints:

$$\prod_{c\in C_r} B_c^X = \prod_{c\in C_g} B_c^X = \prod_{c\in C_b} B_c^X = \prod_{c\in C_y} B_c^X, \quad (15)$$

where C_p is the set of p-cells. They imply that the number of quasiparticles of each color must agree in their evenness or oddness. Therefore, if we want to create quasiparticles of a single color from the vacuum we must create them in pairs, and so such a creation can be performed with an open string operator. Alternatively, 4 quasiparticles, one of each color, can also be created locally, see Fig. 12 (b). For example, let $|\psi\rangle$ be a ground state and i any site. Then the state $Z_i|\psi\rangle$ is an state with four quasiparticle excitations, one at each of the 3-cells that meet at site i. Observe that (15) is in agreement with (10).

Now let $|\psi\rangle$ be a ground state and let M_b^{gy} be a membrane operator which has a boundary ∂b. Recall that ∂b is a set of edges in the gy-shrunk complex that corresponds to a set of rb-faces at the colex level. The state $M_b^{gy}|\psi\rangle$ is an excited state with excitations placed at the faces in ∂b. The excited segments, as viewed in the gy-shrunk complex, form a closed path. This motivates the idea of a gy-flux in the boundary of the membrane, as illustrated in Fig.13 for a membrane with a single face. But we have to check that this flux makes sense. Not only it must be conserved at any vertex in the gy-shrunk graph, but also the existence of fluxes of other colors must be considered. So take for example a r-cell c. We have 2 constraints for the faces of c, analogous to those in (15) but in the subcolex that forms the boundary of c:

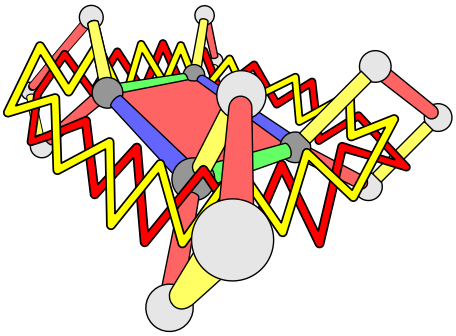

FIG. 13: The flux excitation created with the membrane operator B_m^X of a ry-membrane made up of a single ry-face.

$$\prod_{f\in F_{rb}^c} B_f^Z = \prod_{f\in F_{rg}^c} B_f^Z = \prod_{f\in F_{rb}^c} B_f^Z, \quad (16)$$

where F_{pq}^c is the set of pq-faces of the cell c. These constraints guarantee that gy-flux is preserved at the corresponding vertex in the gy-shrunk complex. Additionally, (16) imply that a gy-flux can split in a gb-flux plus a yb-flux, see Fig. 14 (b). This is of course in agreement with (11).

Fluxes can be analyzed from a different point of view. Let $|\psi\rangle$ be a ground state and i any site. Then the state $X_i|\psi\rangle$ is an excited state. We can visualize it as small p-fluxes winding around the p-edges incident at i, as shown in Fig. 14 (c). Observe that the idea of a pq-flux as something composed of a p-flux and a q-flux is also suggested by the flux splitting (16). Any flux configuration is a combination of these microfluxes at sites. In particular, the total flux through any closed surface must be null, and thus we cannot have, for example, an isolated rg-flux in a loop which is not homologous to zero.

F. Winding quasiparticles around fluxes

In the theory of topological order in 2D it is known that quasiparticles show special statistics [51], [52]: when a charge is carried around another one, sometimes the system gets a global phase, a behavior which bosons and fermions do not show. Which is the analogous situation in 3D? We can carry a charged particle along a closed path which winds around a loop of flux, as in Fig. 15. If the system gets a global phase, then it makes sense to introduce the notion of branyons as the higher dimensional generalization of the usual anyons. Thus in the system at

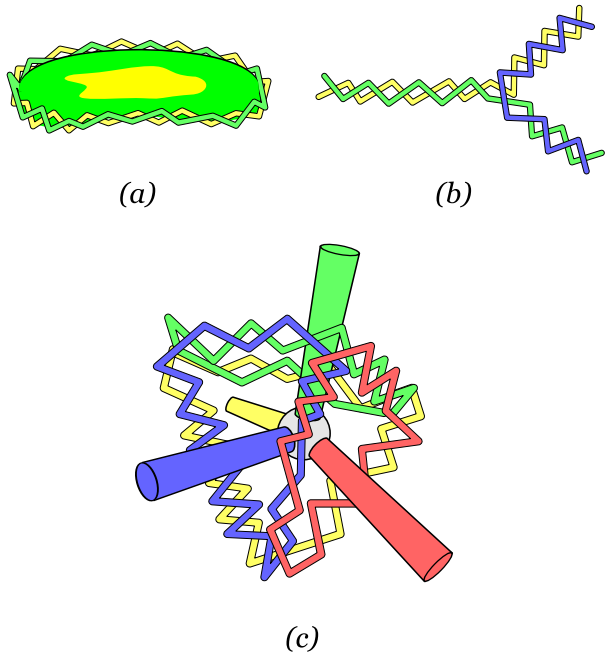

FIG. 14: (a) The border of a gy-membrane is a gy-flux. (b) A gy-flux can split in a gb-flux and a by-flux when it goes across a r-cell (16). (c) The microfluxes at a given site, as explained in the text.

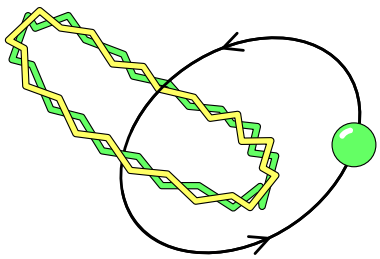

FIG. 15: When a g-charge winds around a loop of gy-flux the system gets a global -1 phase. This is because the membrane operator giving rise to the flux and the string operator associated to the winding anticommute.

hand we have 0-branyons (quasiparticles) and 1-branyons (fluxes). Higher dimensional branyons will appear when we consider systems with $D \geq 4$.

In order to see the effect of winding a color charge around a color flux, we have to consider the closed string operator associated to the charge path and the membrane giving rise to the flux loop. If a p-charge winds once around a pq-flux, the system will get a global -1 phase because $\{M^{pq}, S^p\} = 0$. Observe that this reinforces the idea of a pq-flux as a composition of a p-flux and a q-flux. Other color combinations, i.e., those in which string and membrane do not share a color, give no phase.

III. D-COLEXES

In order to generalize the 3-dimensional model to higher dimension D we have first to construct the underlying structure. That is, we want to define color complexes of arbitrary dimension. This section is devoted to the definition and basic properties of D-colexes.

A. Definitions

First we define color graphs or *c-graphs*. A v-valent c-graph is a graph Γ satisfying that
(i) v edges meet at every vertex,
(ii) edges are not loops and
(iii) edges are v-colored.
For being v-colored we mean that labels from a color set $Q = \{q_1, \ldots, q_v\}$ have been assigned to edges in such a way that two edges meeting at a vertex have different colors. This is a generalization of what we already saw in the $D = 3$ case, as in Fig. 4. A c-graph Γ' with color set Q' is a c-subgraph of Γ if $\Gamma' \subset \Gamma$, $Q' \subset Q$ and the colorings coincide in common edges.

Now we introduce *complexes*. One can give to a D-manifold a combinatorial structure by means of what is called a D-complex. The idea is to divide the manifold in a hierarchy of objects of increasing dimension: points, edges, faces, solid spheres, etc. These objects are called n-cells, $n = 0, \ldots, D$. 0-cells are points, 1-cells are edges, and so on. The boundary of a n-cell is a n-sphere and is made up of cells of dimension $n' < n$. So what we have is a D-manifold constructed by gluing together the higher dimensional analogs of the polihedral solids that we considered in $D = 3$, recall Fig. 2.

A D-colex is a complex in a D-manifold which has $(D+1)$-colored edges in such a way that
(i) its underlying lattice or graph is a (D+1)-valent c-graph,
(ii) the subgraph that lyes on the boundary of any n-cell for $n = 2, \ldots, D$ is a n-valent c-subgraph and
(iii) any connected c-subgraph with valence $v = 2, \ldots, D$ lyes on the boundary of one unique v-cell.
Therefore the point is that the c-graph *completely* determines the cell structure and thus the whole topology of the manifold.

Some c-graphs yield a colex, but not all of them. We define recursively this partially defined mapping from the space of $(D+1)$-valent c-graphs to the space of closed D-manifolds. First, any 2-valent c-graph is a collection of loops, so as a topological graph it naturally yields a 1-manifold, namely a collection of 1-spheres. Then consider any 3-valent c-graph. We construct a 2-complex starting with the corresponding topological graph or 1-complex. The idea is first to list all 2-valent c-subgraphs, which are embeddings of S^1 in the 1-complex. Then for each of these subgraphs we attach a 2-cell, gluing its boundary to S^1. The resulting space is certainly a 2-manifold. It is enough to check a neighborhood of any vertex, but the

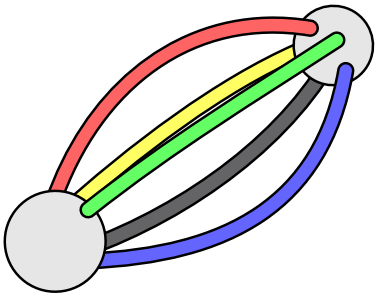

FIG. 16: A c-graph that yields a 4-sphere. It is the simplest possible 4-colex, with only two vertices.

one to one correspondence between cells and connected c-subgraphs makes this straightforward. Then we consider a 4-valent c-graph. If not all of its 3-valent c-subgraphs yield S^2, we discard it. Otherwise we first proceed to attach 2-cells as we did for the 3-valent graph. Then we list all 3-valent c-subgraphs, which by now correspond to embeddings of S^2 in a 2-complex. At each of these spheres we glue the surface of a solid sphere. The process can be continued in the obvious way and thus in general a $(D+1)$-valent c-graph yields a D-colex iff all its D-valent c-subgraphs yield S^D.

B. Examples

As a first example of colex, consider the c-graph composed of only two vertices, for any valence $v = D+1 \geq 2$. An example can be found in Fig. 16. This family of c-graphs yields the spheres S^D. This can be visualized viewing S^D as $\mathbf{R}^D$ plus the point at infinity. We can place one vertex at the origin and the other at infinity. Then edges are straight lines that leave the origin in different directions.

The projective space P^D can also be described easily with a colex, though less economically in terms of vertices. Recall that P^D can be constructed by identifying opposite points of the boundary of a D-dimensional ball. The idea is to consider a D-cube and construct a D-valent c-graph with its vertices and edges, coloring parallel edges with the same color. Then we add 2^{n-1} extra edges to connect opposite vertices, and give them a new color. The resulting c-graph yields P^D. See Fig. 5 for an example in the case $D = 3$.

In appendix B we give a procedure to construct colexes from arbitrary complexes. This guarantees that we can construct our topologically ordered physical system in any closed manifold with $D \geq 2$.

C. R-shrunk complex

This section is devoted to the construction of several new complexes from a given colex. These constructions will be essential for the understanding of the physical models to be built. In particular, as we learnt in the $D = 3$ case, only at the shrunk complex level will it be possible to visualize neatly the branes that populate the system. Shrunk complexes also provide us with several relations among the cardinalities of the sets C_n of n-cells, which in turn will be essential to calculate the degeneracy of the ground state. These relations are based on the Euler characteristic of a manifold, a topological invariant defined in a D-complex as:

$$\chi := \sum_{n=0}^{D} (-1)^n |C_n| \tag{17}$$

Before starting with the construction, it is useful to introduce the notion of the Poincaré dual of a complex $\mathcal{C}$ in a D-manifold. The dual complex $\mathcal{C}^*$ is obtained by transforming the n-cells of $\mathcal{C}$ in $(D-n)$-cells, and inverting the relation being-a-boundary-of. This means that if certain $(n-1)$-cell c' is in the boundary of the n-cell c in $\mathcal{C}$, then c^* is in the boundary of c'^* in $\mathcal{C}^*$.

We say that a cell is a R-cell if its c-graph has as color set R. Note that this notation is different from the one we used in $D = 3$, but it is more suitable for high D. What before was a gy-membrane now will be a $\{r, b\}$-brane, or more simply a br-brane, and so on.

Consider a D-colex $\mathcal{C}$ with color set Q. We want to construct its R-shrunk complex $\mathcal{C}_R$, where R is a nonempty proper subset of Q, $\emptyset \subsetneq R \subsetneq Q$. What we seek is a new complex in which only R-cells remain whereas the rest of $|R|$-cells disappear. This construction is accomplished by a partial Poincaré dualization of cells. We already saw examples of this construction in $D = 3$. Due to the different notation, a gy-shrunk complex there will be a rb-shrunk complex here.

The R-shrunk complex has two main sets of cells. The first one corresponds to the cells in the set

$$S_1 := \bigcup_{R \subseteq S \subsetneq Q} C_S, \tag{18}$$

where C_S is the set of S-cells. Cells in S_1 keep their dimension and the relation being-the-boundary-of among them. The second cell set is

$$S_2 := \bigcup_{\bar{R} \subseteq S \subsetneq Q} C_S, \tag{19}$$

where $\bar{R}$ is the complement of R in Q

$$\bar{R} := Q - R. \tag{20}$$

Cells in S_2 get dualized. This means that a n-cell in the colex will be a $(D-n)$-cell in the R-reduced complex. The relation being-the-boundary-of is inverted among the cells in S_2. So S_2 provides us with cells of dimensions $0, \ldots, |R|-1$ and S_1 with cells of dimensions $|R|, \ldots, D$. Up to dimension $|R|-1$ the construction is clear, but we have to explain how to attach the cells in S_1. To this end, we observe that the intersection of a n-cell in S_1 and a

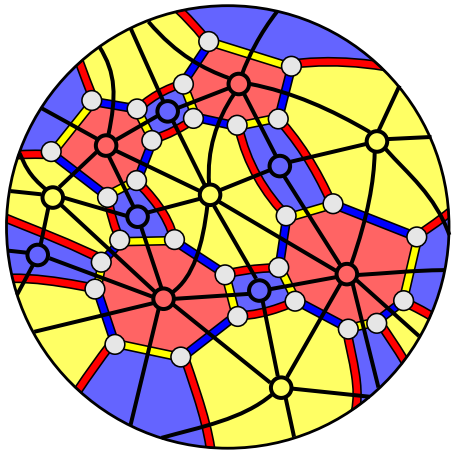

FIG. 17: A *bry*-cell belonging to some D-colex with $D \geq 3$. Superimposed we show in black thick line the structure of its dual boundary, which plays an important role when constructing the *bry*-shrunk complex.

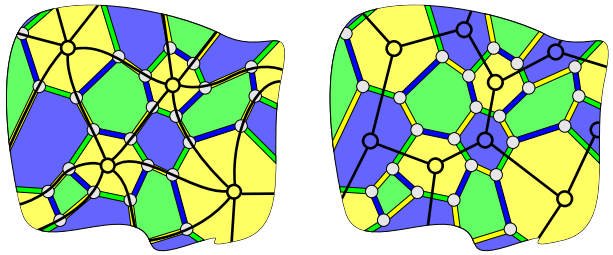

(a) (b)

FIG. 18: This figure shows the two possible kinds of shrunk complex in a 2-colex. The shrunk complexes appear superimposed in black thick line to the original colex. In (a) it is shown the y-shrunk complex, and in (b) the *by*-shrunk complex.

R-cell is either empty or a cell of dimension $n' = n - |\bar{R}|$. The n-cell gives rise to a cell of dimension $D - n = |R| - 1 - n'$. Thus, the partial dualization is in fact a complete dualization as seen on the boundary of any R-cell, and the attachment of each R-cell is then naturally described by this dualization process, as shown in Fig. 17. For the cells coming from S-cells with $R \subsetneq S$ the attachment can be described recursively. The boundary of these cells is a $(|S|-1)$-colex, so we can obtain its R-shrunk complex and use it as the new boundary for the cell. In fact, what we are doing is a projection of the shrunking process in the boundary of the cell. Fig. 18 displays examples of shrunk complexes for $D = 2$.

The Euler characteristic for a R-shrunk complex is

$$\chi = \sum_{R \subseteq S \subsetneq Q} (-1)^{|S|} |C_S| + \sum_{\bar{R} \subseteq S \subsetneq Q} (-1)^{D-|S|} |C_S|. \quad (21)$$

If we sum up all such equations for all different color combinations but fixed cardinality $|R| = r$ we get

$$\binom{D+1}{r}\chi = \sum_{n=r}^{D} (-1)^n \binom{n}{r} |C_n| + \\ + \sum_{n=0}^{r-1} (-1)^n \binom{D-n}{D-r+1} |C_{D-n}|. \quad (22)$$

The case $r = 0$ is also included since it reduces to the definition of χ. The rhs are equal in the cases $r = s$ and $r = D - s + 1$ except for a sign, so that we get

$$\chi = (-1)^D \chi. \quad (23)$$

Of course, this is the well known fact that χ vanishes in manifolds of odd dimension. In these cases in which $D = 2k + 1$, equation (22) for $r = k + 1$ vanishes identically. So in general we have $\lceil D/2 \rceil$ independent relations. They tell us that the cardinalities $|C_0|, \ldots, |C_{\lfloor D/2 \rfloor}|$ depend of the cardinalities $|C_{\lfloor D/2+1 \rfloor}|, \ldots, |C_D|$, which shows quantitatively the fact that colexes are much more 'rigid' than more general complexes.

IV. THE MODEL IN D-MANIFOLDS

A. System and Hamiltonian

We now associate a physical system to a D-colex structure in a D-manifold, $D \geq 2$. To this end, we place at each vertex (site) a spin-$\frac{1}{2}$ system. To each n-cell c we can attach the cell operators

$$B_c^\sigma := \bigotimes_{i \in I_c} \sigma_i, \qquad \sigma = X, Z \quad (24)$$

where X_i and Z_i are the Pauli σ_1 and σ_3 matrices acting on the spin in the vertex i and I_c is the set of vertices lying on the cell c. In order to generalize the Hamiltonian (4) we need sets of cells such that their X and Z operators commute. But we have the following result. For every n-cell c_n and m-cell c_m with $n + m > D + 1$

$$[B_{c_n}^X, B_{c_m}^Z] = 0. \quad (25)$$

This is a consequence of the fact that c_n and c_m have colexes with at least one color in common, because they have respectively $p + 1$ and $(q + 1)$ colors. Then their intersection is a colex of valence at least 1, and thus contains an even number of sites.

From this point on we choose fixed integers $p, q \in \{1, \ldots, D-1\}$ with

$$p + q = D. \quad (26)$$

The Hamiltonians that we propose is

$$H_{p,q} = -\sum_{c \in C_{p+1}} B_c^Z - \sum_{c \in C_{q+1}} B_c^X \quad (27)$$

Again, color plays no role in the Hamiltonian. It is an exactly solvable system and the ground state corresponds to a quantum error correcting code with stabilizer the set of cell operators[53]. We give a detailed calculation of the degeneracy in appendix D. The degeneracy is 2^k with

$$k = \binom{D}{p} h_p = \binom{D}{q} h_q, \tag{28}$$

where $h_p = h_q$ is the p-th Betty number of the manifold. The ground states $|\psi\rangle$ are characterized by the conditions

$$\forall\, c \in C_{p+1} \qquad B_c^Z |\psi\rangle = |\psi\rangle, \tag{29}$$

$$\forall\, c \in C_{q+1} \qquad B_c^X |\psi\rangle = |\psi\rangle. \tag{30}$$

Those eigenstates $|\psi'\rangle$ for which some of these conditions are violated are excited states. As in the $D = 3$ case, excitations have a local nature and we have a gapped system.

As a new feature respect to the three dimensional case, for $D \geq 4$ different combinations of the parameters (p, q) are possible. Each of these combinations gives rise to different topological orders, thus making possible transitions between them. For example, in $D = 4$ the Hamiltonian

$$H = H_{1,3} + \lambda H_{2,2} \tag{31}$$

exhibits a topological phase transition as λ is varied.

B. Branes

In analogy with the string and membranes that appeared in the $D = 3$ case, here we have to consider p-branes. For a p-brane we mean an embedded p-manifold, closed or with a boundary. A p-brane is homologous to zero when it is the boundary of a $p+1$-brane. Then two p-branes are homologous if the p-brane obtained by their combination is homologous to zero.

Let Q be as usual the set of colors of the D-colex. Then for any nonempty set $R \subsetneq Q$, a R-brane is a collection of R-cells. It can be truly visualized as a $|R|$-brane in the R-shrunk complex. There we see also that its boundary corresponds to $\bar{R}$ cells. Let b be a R-brane and C_b its set of R-cells. Then we can attach to b operators $B_b^\sigma := \prod_{c \in C_b} B_c^\sigma$ for $\sigma = X, Z$. Suppose in particular that $|R|$ = p and let b be a closed R-brane. Then B_b^Z commutes with the Hamiltonian. If this were not the case, then it would exist a $(q+1)$-cell, in particular an $\bar{R}$-cell c, such that $\{B_b^Z, B_c^X\} = 0$. But in that case, in the R-shrunk complex the p-brane would have a boundary at the cell coming from c. Similarly, closed q-brane X operators also commute with the Hamiltonian.

The operator B_c^Z of a $(p+1)$-cell c with color set $R \cup \{r\}$, $r \in Q - R$, is a closed R-brane. As the R-shrunk complex reveals, it corresponds to the boundary of c. B_c^Z acts trivially in ground states (29), and the same holds true for any closed p-brane homologous to zero since it is a combination of such operators B_c^Z. This is not the case for closed p-branes which are not homologous to zero, and thus they act nontrivially in the ground state.

1. Equivalent branes

It is natural to introduce an equivalence among those operators of the form $\bigotimes_{v \in V} Z_v^{i_v}$, where V is the set of vertices of the colex and $i_v \in \{0, 1\}$. We say that two such operators O_1 and O_2 are equivalent, $O_1 \sim O_2$, if $O_1 O_2$ is a combination of $(p+1)$-cell operators B_c^Z. This induces an equivalence among p-branes, since they have such an operator attached. In fact, two R-branes b and b', with $|R| = p$, are equivalent if and only if they are homologous. Observe that two equivalent p-brane Z operators produce the same result when applied to a ground state. This motivates the introduction of the notation P_μ^R, $|R| = p$, for any operator B_b^Z with b a R-brane with homology labeled by μ.

Likewise, we can introduce an equivalence among those operators of the form $\bigotimes_{v \in V} X_v^{i_v}$ just as we have done for Z operators. This induces an equivalence relation among q-branes, and we use the notation Q_ν^R, $|R| = q$, for any q-brane operator B_b^X with b a R-brane with homology labeled by ν.

In appendix C we show that for any color set $R \subset Q$ with $|R| = p - 1$

$$\prod_{r \in Q - R} P_\mu^{rR} \sim 0, \tag{32}$$

where rR is a shorthand for $\{r\} \cup R$. Similarly if $|R| = q - 1$

$$\prod_{r \in Q - R} Q_\mu^{rR} \sim 0. \tag{33}$$

These relations generalize (10) and (11). They give the interplay between homology and color, and show that for each homology class only $\binom{D}{p}$ color combinations are independent, those which can be formed without using one of the $D+1$ colors. This is why a combinatorial number appears in the degeneracy of the ground state. The other factor, h_p, follows from the fact that a homology basis for p-branes has h_p elements. Using the theory of quantum stabilizer codes[53] one can see that by selecting a basis for p-branes with labels $\mu = 1, \ldots, h_p$ and a color r we can form a complete set of observables $\{P_\mu^R\}_{\mu, R \not\ni r}$.

2. Commutation rules

In general for suitable color sets R, S we have

$$R \cap S \neq \emptyset \quad \Rightarrow \quad [P_\mu^R, Q_\nu^S] = 0. \tag{34}$$

This follows from the same reasoning used in (25). We now explore the situation when R and S have no color

in common. Consider a basis $\{p_\mu\}$ for closed p-branes. Consider also a basis for q-branes $\{q_\nu\}$, but chosen so that p_μ and q_ν cross once if $\mu = \nu$, and do not cross in other case. Then

$$R \cap S = \emptyset \quad \Rightarrow \quad P^R_\mu Q^S_\nu = (-1)^{\delta_{\mu,\nu}} Q^S_\mu P^R_\nu. \tag{35}$$

This can be reasoned without resorting to the geometrical picture. Suppose that $[P^R_\mu, Q^S_\mu] = 0$ and let $R = R' \cup \{r\}$, $Q - R - S = \{q\}$. From (32) we have $[\prod_{r'} P^{R'r'}_\mu, Q^S_\mu] = 0$. Then (34) implies $[P^{Rq}_\mu, Q^S_\mu] = 0$, and thus we have a homologically nontrivial q-brane X operator that commutes with all the p-brane Z operators. This being impossible, the assumption is necessarily false.

C. Excitations

There are two kinds of excitations, depending on wether a $(p+1)$-cell or a $(q+1)$-cell condition is violated. We label excitations with the color set of the cell they live in. Although we focus on violation of $(q+1)$-cells, the situation is analogous for $(p+1)$-cells.

Let $|\psi\rangle$ be a ground state and b a R-brane, $R \subset Q$, $|R| = p$. We first observe that b has a boundary in the R-shrunk complex at the cell corresponding to the $\bar{R}$-cell c iff

$$\{P^R_b, B^X_c\} = 0. \tag{36}$$

But $B^Z_b|\psi\rangle$ has $\bar{R}$-excitation exactly at those cells fulfilling (36). These means that the excitation produced by the p-brane b has the form of a $p-1$-brane, precisely the boundary of b, ∂b.

Consider the particular case $p = 1$. The excitations living at D-cells are, as in the $D = 3$ case, quasiparticles (anyons) with color charge. In a connected manifold, we have D constraints generalizing (15). They have the form

$$\prod_{c \in C_R} B^X_c = \prod_{c \in C_S} B^X_c, \tag{37}$$

where $|R| = |S| = D$ and C_R is the set of R-cells. These relations imply that the number of particles of each color must agree in their parity. Therefore, from the vacuum we can create pairs of particles of a single color or groups of $D+1$ particles, one of each color. This is completely anologous to $D = 3$.

Now suppose that $p > 1$. We have seen that excitations can be created as the boundary of a p-brane. If in particular it is a R-brane, then excitations live in $\bar{R}$-cells. It is natural an interpretation of these excitations as some kind of $(p-1)$-dimensional flux, a $\bar{R}$-branyon. Then it must be conserved, and in fact for each $(q+2)$-cell c we have the constraints:

$$\prod_{c \in C^c_R} B^X_c = \prod_{c \in C^c_S} B^X_c, \tag{38}$$

where $|R| = |S| = q+1$ and C^c_R is the set of R-cells lying on the cell c. This is a generalization of (16) and is in agreement with (32).

Finally, as in the 3-dimensional case, we can wind branyons around each other and sometimes get a global phase. Let $|R| = q+1$ and $|S| = p+1$. Then when a R-branyon winds around a S-branyon, the system gets a global minus sign iff $|R \cap S| = 1$, as follows from the commutation rules (35).

V. CONCLUSIONS

In this paper we have explored topological orders in $D = 3$ by means of models for quantum lattice Hamiltonians constructed with spins $S = \frac{1}{2}$ located at lattice sites. These models are exactly solvable and this is a feature that allows us to explore the quantum properties of the whole spectrum. The ground state is found to be in a string-net condensate, or alternatively in a membrane-net condensate. This type of membrane-net condensation is an interesting feature of our models that do not appear in 3D toric codes. In dimensions higher than $D = 3$ we have also extended the construction of our models and found brane-net condensation. As for excitations, they are either quasiparticles or certain type of extended fluxes. These excitation show unusual braiding statistics properties similar to anyons in $D = 2$, and we call them branyons since they involve extended objects associated to branes.

Another interesting result is the possibility of having a topology-changing transition between two topologically ordered phases that we find with our models in $D = 4$. We may wonder whether it is possible to have a similar topology-changing process in dimension $D = 3$ as in (31). One obvious way to achieve this is by using the construction in $D = 4$ and flatten it into $D = 3$, thereby reducing the dimensionality of the interaction but at the expense of loosing the locality of the interaction.

There does not exist a fully or complete topological order in $D = 3$ dimensions, unlike in $D = 2$. That is to say, there does not exist a topological order that can discriminate among all the possible topologies in three dimensional manifolds. We may introduce the notion of a Topologically Complete (TC) class of quantum Hamiltonians when they have the property that their ground state degeneracy (and similarly for excitations) is different depending on the topology of the manifold where the lattice is defined on. From this perspective, we have found a class of topological orders based on the construction of certain lattices called colexes that can distinguish between 3D-manifolds with different homology properties. Homology is a topological invariant, but not enough to account for the whole set of topologically inequivalent manifolds in $D = 3$. For instance, the famous Poincaré sphere is an example of 3D-manifold that has the same homology as a 3-sphere. Poincaré was able to proof that the fundamental group (or first homotopy

group) of this new sphere has order 120. As the standard 3-sphere has trivial fundamental group, they are different. Since then, many other examples of homology spheres have been constructed that are different topological structures. In this regard, we could envisage the possibility of finding a quantum lattice Hamiltonian, possibly with a non-abelian lattice gauge theory, that could distinguish between any topology in three dimensions by means of its ground state degeneracy. This would amount to solving the Poincaré conjecture with quantum mechanics.

From the viewpoint of quantum information, the topologically ordered ground states that we have constructed provide us with an example of topological quantum memory: a reservoir of states that are intrinsically robust against decoherence due to the encoding of information in the topology of the system.

Acknowledgements We acknowledge financial support from a PFI fellowship of the EJ-GV (H.B.), DGS grant under contract BFM 2003-05316-C02-01 and INSTANS (M.A.MD.), and CAM-UCM grant under ref. 910758.

APPENDIX A: CONNECTED SUM

This appendix is not strictly necessary in the logical structure of the text, but we include it because it gives a beautiful example of how the topological structure of a colex is contained in its c-graph.

Given two connected D-manifolds $\mathcal{M}_1$ and $\mathcal{M}_2$, their connected sum is constructed as follows. First choose a pair of D-discs, one in each manifold, and delete its interior. Then we glue together their boundaries. The resulting object is a D-manifold, denoted $\mathcal{M}_1\sharp\mathcal{M}_2$.

As we have already noted, a c-graph contains all the information about its manifold, if it yields any. Thus one expects that the connected sum of two manifolds can also be expressed in terms of c-graph manipulations. In fact, this is true, as we explain now.

Consider two D-colexes, $\mathcal{C}_1$ and $\mathcal{C}_2$. In order to construct $\mathcal{C}_1\sharp\mathcal{C}_2$, we choose a vertex of each of the colexes and select small neighborhoods of these vertices. Due to the one-to-one correspondence between c-graphs and cells, this two neighborhoods of vertices are identical at a complex and color level. Thus the gluing operation between boundaries can be chosen so that the structure of the complex is preserved and the coloring of edges coincides. Therefore, the result of the operation is a D-colex.

How do we express the process at a c-graph level? Simply choose one vertex at each c-graph, and delete them. Then connect the edges according to their color. Fig. 19 displays the procedure.

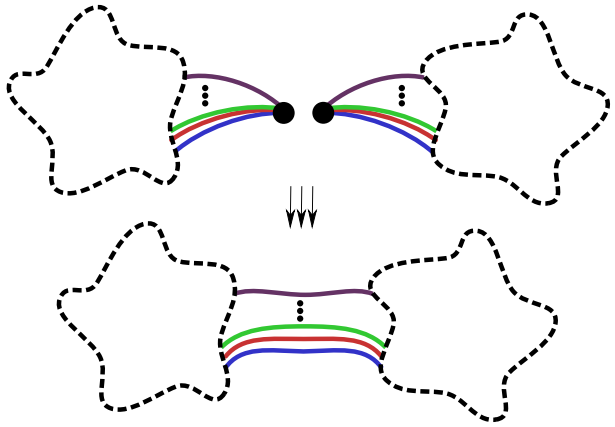

FIG. 19: The connected sum of two colexes can be performed at a c-graph level. Two vertexes must be selected and deleted. Then the edges that have been cut must be joined according to their color.

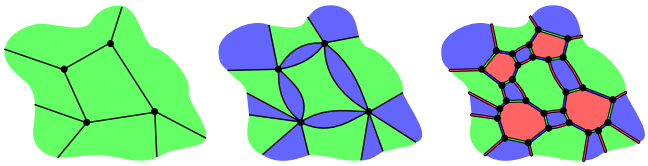

FIG. 20: This figure explains a process that converts an arbitrary 2-complex on a surface into a 2-colex. In (a) green color is given to all the 2-cells of the 2-complex. In (b) 1-cells are inflated to give blue 2-cells. Finally in (c) 0-cells are inflated to give red 2-cells and 1-cells are accordingly colored.

APPENDIX B: HOW TO CONSTRUCT D-COLEXES

We present a procedure to construct colexes in arbitrary closed manifolds. The idea is to start with an arbitrary complex and inflate its cells till a colex is obtained. We now explain the process in detail. It is illustrated in Fig. 20.

First we have to state what we mean by inflating a n-cell, $0 \leq n \leq D$. The idea is to preserve the boundaries of the cell untouched but inflate all other points in order to obtain a D-cell. For each $(n+l)$-cell that belongs to the boundary of the inflated cell, we must introduce a $(n+l-1)$-cell. The inflation of cells of the same dimension can be performed in any order, and all the cells must be inflated. Inflation starts with $(n-1)$-cells, then continues with $(n-2)$-cells, and so on, till 0-cells are inflated in the end.

We can proof that this procedure gives a D-colex by an inductive argument. We will need some facts. First, we observe that the D-cells of a D-colex can be labeled with the unique color which its subcolex does not contain. Conversely, if we can color the D-cells of a D-colex with $D+1$ colors in such a way that neighboring cells have different colors, then we can color edges according

to the D-cells they connect. Note also that for each cell in the original D-complex, the inflated one has a D-cell. This means that we can label inflated D-cells with the dimension of the cell in the original complex.

Finally we proceed with the proof. The case $D = 1$ is trivial. We suppose that the procedure works for (D)-manifolds, and check it for $(D + 1)$-manifolds. To this end, consider the boundary of any inflated $(D + 1)$-cell which comes from the inflation of a 0-cell. Imagine all the inflation process projected into this (fixed) D-sphere. In the beginning, we can see a complex in this sphere. Its vertices correspond to edges that cross the surface, edges to faces that cross it, and so on. As the inflation proceeds in the original complex, the projected complex is also inflated. When 1-cells are inflated, the projected complex has become a D-colex because of the induction hypothesis. Thus it can be properly colored. Moreover, we can perform the coloring on its D-cells using the labels attached to the corresponding $(D + 1)$-cells in the inflated $(D + 1)$-complex. From this coloring we deduce a coloring for the edges of the D-colex. In fact, all this is true for each of the subgraphs in the surfaces of $(D + 1)$-cells obtained by inflation of 0-cells. Finally, we give a different color to the edges that are not contained in these surfaces. Checking that this coloring gives the desired properties that make the complex a colex is now easy.

APPENDIX C: BRANE COMBINATION

Consider a D-colex with color set Q. Let b_R be a closed R-brane, $\emptyset \subsetneq R \subsetneq Q$. It is the purpose of this section to show that for any $r \in R$ there exist a family of closed $|R|$-branes b_S homologous to B_R such that

$$B^\sigma_{b_R} = \prod_S B^\sigma_{b_S}. \tag{C1}$$

The sum extends over all $S \subset \bar{r} := Q - \{r\}$ with $|S| = |R|$.

We first consider the case $R = \{r\}$. Then b_R is a string. It consists of r-egdes that link $\bar{R}$-cells. $B^\sigma_{b_R}$ acts nontrivially in an even number of vertices per $\bar{R}$-cell. Thus we can gather them together in pairs, and connect them through a path which only contains edges with colors in $Q - R$. Then for each $s \in Q - R$, the set of all s-edges we have used forms a string b_S, $S = s$. Then, certainly (C1) holds true and each string b_S is closed because the r.h.s. commutes with operators from $\bar{S}$ cells and so the l.h.s. also does.

Now consider the case $|R| > 1$. Let $\tilde{r} := R - \{r\}$. Consider the restriction of $B^\sigma_{b_R}$ to any $\bar{r}$-cell c, denoted B^σ_b. This operator corresponds to a closed $\tilde{r}$-brane b in the $(D - 1)$-colex that forms the boundary of c. Since this colex is a sphere, b is a boundary and thus B^σ_b is a combination of $|R|$-cells. As we did for strings, we can do this for every $\bar{r}$-cell, gather cells together by color and form the required closed $|R|$-branes.

APPENDIX D: DEGENERACY OF THE GROUND STATE

In the theory of quantum error correcting codes, the ground state of the Hamiltonian (27) is called a stabilizer code [53]. Thus, the theory of stabilizer codes naturally fits to study the degeneracy, but we will avoid to use its language although this makes the exposition less direct.

The ground state of the Hamiltonian (27) is the intersection of subspaces of eigenvalue 1 of $(p + 1)$-cell and $(q+1)$-cell operators, as expressed in equations (29) and (30). This subspace has an associated projector, which in turn will be the product of the projectors onto each of the subspaces of eigenvalue 1:

$$\prod_{c\in C_{p+1}} \frac{1}{2}(1 + B^Z_c) \prod_{c\in C_{q+1}} \frac{1}{2}(1 + B^X_c). \tag{D1}$$

Each of these projectors reduces the dimension of the space by a half, but not all of them are independent, because certain relations among cell operators exist. For $(p + 1)$-cells these relations have the form

$$\prod_{c\in C_{p+1}} (B^Z_c)^{i_c} = 1, \tag{D2}$$

where $i_c = 0, 1$. Analogous relations exist for $(q+1)$-cells:

$$\prod_{c\in C_{q+1}} (B^X_c)^{i_c} = 1. \tag{D3}$$

If the number of spins is n and the number of independent projectors is l, then the degeneracy of the ground state will be 2^k with $k = n - l$. Suppose that the number of independent relations of type (D2) is l_1 and that for relations (D3) this number is l_2. Then we have $l = |C_{p+1}| - l_1 + |C_{q+1}| - l_2$. Our starting point is then the equation

$$k = |C_0|-|C_{p+1}|-|C_{q+1}|+I(D,p+1)+I(D,q+1), \tag{D4}$$

where $n = |C_0|$ is the number of sites and $I(D, s)$ is the number of independent relations among s-cells in a D-colex.

$I(D, s)$ only depends upon the cardinalities of cell sets $|C_i|$ and the Betty numbers of the manifold h_i, as we will show calculating its value recursively. First, we note that

$$I(D, D) = dh_0, \tag{D5}$$

because the unique independent relations in this case are those in (37), for each connected component. For $s < D$, a relation between cells has the general form

$$\prod_{|S|=s} \prod_{c\in D_S} B^\sigma_c = 1, \tag{D6}$$

where $D_S \subset C_S$. Let $r \in Q$ be a color. If we only consider those relations that include color sets $R \subset \bar{r}$ we

effectively reduce the problem by 1 dimension. Gathering together all such relations that appear in $\bar{r}$-cells we get a total count of

$$I_{\bar{r}}(D,s) = I(D-1,s)|_{h_0=h_D=|C_{\bar{r}}|, h_{i\neq 0,D}=0}. \qquad \text{(D7)}$$

Since the r.h.s. of (D6) commutes with any cell operator, in fact the relation has the form

$$\prod_{|S|=s} B^{\sigma}_{b_S} = 1, \qquad \text{(D8)}$$

where b_S is a *closed* S-branes b_S. Then consider any such relation in which a R-brane b_R appears with $r \in R$. If we have at hand all the relations of the form (C1), we can use them to eliminate the term b_R in (D8). This can be done for every such R, till a relation containing only colors in $\bar{r}$ is obtained. Therefore, our following task is to count how many of the relations (C1) are independent for each R.

Suppose then that we have a relation of the form (C1) that follows from other t relations of the same form (but not from a subset of them):

$$B^{\sigma}_{b_{R,i}} = \prod_S B^{\sigma}_{b_{S,i}} \qquad i = 1,\ldots,t. \qquad \text{(D9)}$$

Then for the l.h.s of the relations the following is true

$$B_{b_R} = \prod_{i=1}^{t} B_{b_{R,i}}. \qquad \text{(D10)}$$

Since all the branes that appear in (C1) are R-branes, the equation can be interpreted in terms of Z_2-chains of $|R|$-cells in the R-shrunk complex. It states that $b_R = b_{R,1} + \cdots + b_{R,t}$. The argument can be reversed; any such a dependence between $|R|$-cycles in the R-shrunk complex corresponds to a dependence among relations of the form (C1).

Therefore, counting the number of independent relations of the form (C1) for a given R amounts to count the number of independent $\mathbf{Z}_2$-chains of closed $|R|$-cycles in the R-shrunk complex. For $|R| = s$, this number is

$$S(D,s) = \sum_{i=0}^{n-s}(-1)^i h_{s+i} + \sum_{i=1}^{n-s}(-1)^i |C_{s+i}|. \qquad \text{(D11)}$$

This follows by recursion. $S(D,D) = h_0$ and $S(D,s) = h_{D-s} + (|C_{s+1}| - S(D,s+1))$.

We have to consider all the possible sets R in which r is contained:

$$I_r(D,s) = \sum_{\substack{R\ni r \\ |R|=s}} S(D,s)|_{R\text{-shrunk}}. \qquad \text{(D12)}$$

Then

$$I(D,s) = I_{\bar{r}}(D,s) + I_r(D,s), \qquad \text{(D13)}$$

which can be solved and gives

$$I(D,s) = \binom{D}{s-1}\sum_{i=0}^{D-s}(-1)^i h_{s+i} + \\ + \sum_{i=0}^{D-s-1}\binom{s+i}{s-1}(-1)^i |C_{s+i+1}| \qquad \text{(D14)}$$

Now recall equations (22). We can sum up these equations for $r = 0,\ldots,s$ with an alternating sign $(-1)^r$. Using the fact that

$$\sum_{i=0}^{a}\binom{b+1}{i}(-1)^i = (-1)^a\binom{b}{a} \qquad \text{(D15)}$$

we get

$$\binom{D}{s}\chi = (-1)^s C_0 + \sum_{i=0}^{s-1}\binom{D-i-1}{D-s}(-1)^i |C_{D-i}| + \\ + \sum_{i=r+1}^{D}\binom{i-1}{s}(-1)^i |C_i|. \qquad \text{(D16)}$$

Gathering together (D4), (D14) and (D16) we finally obtain (28).

[1] L. D. Landau, Phys. Z. Sowjetunion **11**, 26 (1937).
[2] V. L. Ginzburg, L. D. Landau, Zh. Ekaper. Teoret. Fiz. **20**, 1064 (1950).
[3] X.-G. Wen. *Quantum Field Theory of Many-body Systems*, Oxford University Press, (2004).
[4] X.-G. Wen and Q. Niu, Phys. Rev. **B 41**, 9377 (1990).
[5] X.-G. Wen, Int. J. Mod. Phys. **B 4**, 239 (1990).
[6] X.-G. Wen, Int. J. Mod. Phys. **B 6**, 1711 (1992).
[7] A. Kitaev and J. Preskill, Phys. Rev. Lett. **96**, 110404 (2006)
[8] M. Levin and X.-G. Wen, Phys. Rev. Lett. **96**, 110405 (2006).
[9] X.-G. Wen, Phys. Rev. **B 42**, 8145 (1990).
[10] N. Read, Phys. Rev. Lett. **65**, 1502 (1990).
[11] J. Froöhlich and T. Kerler, Nucl. Phys. **B 354**, 369 (1991).
[12] D.S. Rokshar and S.A. Kivelson, Phys. Rev. Lett. **61**, 2376 (1988).
[13] N. Read and B. Chakraborty, Phys. Rev. **B 40**, 7133 (1989).

[14] R. Moessner and S.L. Sondhi, Phys. Rev. Lett. **86**, 1881 (2001).

[15] E. Ardonne, P. Fendley and E. Fradkin, Annals of Phys. **310**, 493 (2004).

[16] V. Kalmeyer and R.B. Laughlin, Phys. Rev. Lett. **59**, 2095 (1987).

[17] X. G. Wen, F. Wilczek, and A. Zee, Phys. Rev. B **39**, 11413 (1989).

[18] N. Read and S. Sachdev, Phys. Rev. Lett. **66**, 1773 (1991).

[19] X.-G. Wen, Phys. Rev. B **44**, 2664 (1991).

[20] Phys. Rev. Lett. **86**, 292 (2001).

[21] X.-G. Wen, Phys. Rev. B **65**, 165113 (2002).

[22] S. Sachdev and K. Park, Annals of Phys. **298**, 58 (2002).

[23] L. Balents, M. P. A. Fisher, and S. M. Girvin Phys. Rev. B **65**, 224412 (2002).

[24] F. Verstraete, M.A. Martin-Delgado, J.I. Cirac, Phys. Rev. Lett. **92**, 087201 (2004).

[25] J. J. Garcia-Ripoll, M. A. Martin-Delgado, J. I. Cirac, Phys. Rev. Lett. **93**, 250405 (2004).

[26] L.-M. Duan, E. Demler, M. D. Lukin, Phys. Rev. Lett. **91**, 090402 (2003), `cond-mat/0210564`.

[27] A. Micheli, G.K. Brennen, P. Zoller, quant-ph/0512222.

[28] J. K. Pachos, quant-ph/0511273.

[29] A. Kitaev, cond-mat/0506438.

[30] A. Galindo and M.A. Martin-Delgado, Rev.Mod.Phys. **74** 347 (2002); quant-ph/0112105.

[31] A. Yu. Kitaev, Annals of Physics **303** no. 1, 2–30 (2003), `quant-ph/9707021`.

[32] M. H. Freedman, Proc. Natl. Acad. Sci., USA, **95** 98-101, (1998).

[33] E. Dennis, A. Kitaev, A. Landahl, J. Preskill, J. Math. Phys. **43**, 4452-4505 (2002).

[34] S. B. Bravyi, A. Yu. Kitaev, quant-ph/9811052.

[35] R. W. Ogburn and J. Preskill, Lecture Notes in Computer Science **1509**, 341–356, (1999).

[36] Michael H. Freedman, Alexei Kitaev, Zhenghan Wang, Commun.Math.Phys. **227** 587-603, (2002).

[37] M. Freedman, M. Larsen, Z. Wang, Comm.Math. Phys. **227** 605–622, (2002).

[38] M. H. Freedman, A. Kitaev, M. J. Larsen, Z. Wang, Bull. Amer. Math. Soc. **40** 31-38, (2003); quant-ph/0101025.

[39] J. Preskill, *Lecture notes on Topological Quantum Computation*, http://www.theory.caltech.edu/preskill/ph219/topological.ps.

[40] H. Bombin and M.A. Martin-Delgado; quant-ph/0605138.

[41] H. Bombin and M.A. Martin-Delgado; quant-ph/0605094.

[42] H. Bombin and M.A. Martin-Delgado, Phys. Rev. A **73**, 062303 (2006); quant-ph/0602063.

[43] W. Thurston, "Three-dimensional geometry and topology". Vol. 1. Edited by Silvio Levy. Princeton Mathematical Series, **35**. Princeton University Press, Princeton, NJ, 1997

[44] G. Perelman, math.DG/0211159.

[45] G. Perelman, math.DG/0303109

[46] G. Perelman, math.DG/0307245

[47] M. Levin and X.-G. Wen, Phys. Rev. **B 71**, 045110 (2005).

[48] A. Hamma, P. Zanardi, X.-G. Wen, Phys.Rev. B **72**, 035307 (2005).

[49] C. Wang, J. Harrington, J. Preskill, Annals Phys. **303** 31-58, (2003).

[50] K. Takeda, H. Nishimori, Nucl. Phys. B **686** 377, (2004)

[51] F. Wilczek, Phys. Rev. Lett. **49**, 957 (1982)

[52] J.M. Leinaas and J. Myrheim, Nuo. Cim. B **37**, 1 (1977).

[53] D. Gottesman, Phys. Rev. A **54**, 1862, (1996).